BEAM LOSS DUE TO MULTIPLE SCATTERING WITH RESIDUAL GASES IN A SLOW ACCELERATING ELECTRON SYNCHROTRON

Y. Gomei*, S. Sukenobu, K. Nakayama
Research and Development Center, Toshiba Corp.
4-1, Ukishima-cho, Kawasaki-ku, Kawasaki Japan

Summary

Beam loss due to multiple scattering with residual gases is studied for a storage-type electron synchrotron where electrons are injected at 15 MeV and accelerated to 800 MeV in 100 s. The temporal behavior of the beam profile was numerically estimated by taking account of damping and the multiple scattering. It was found that almost no beam loss is expected in the horizontal direction, because the adiabatic damping near the inflector wall exceeds the multiple scattering by CO molecules in the pressure of 10^{-9} Torr right after the injection. In contrast, the scattering in the vertical direction is comparable to the adiabatic damping for about 5 s after the injection. The dependency of the beam loss on the vertical aperture (d) was estimated, showing that the beam loss is less than 1% for d=12 mm and 20% for d=7 mm. The duct half height, thus, can be designed to be 15 mm in this respect.

Introduction

Storage-type electron synchrotrons with low energy single multi-turn injection have been studied both experimentally [1] and conceptually [2~4]. The simplicity of this concept appears to be quite attractive in view of industrial application of synchrotron radiation. In case of designing normal conducting machines, it is natural to choose the bending field in the final energy to be about 1.5 T for saving the rf power and for making the machine compact with given requirement on synchrotron radiation. It is also natural to choose the so-called sector-type magnet to increase the bending angle again for compactness of the machine. These selections on the bending magnet design restrict us to use a massive iron core with sufficient return-side cross-section to relieve magnetic saturation. In this case, electrons have to be accelerated slowly to avoid eddy current in the core.

We have studied the Touschek life time [5] and the effect of ion trapping [6] in low electron energy. It has been shown that the life time is long and the tune shift generated by ion trapping is very small because of beam blow-up due to multiple Coulomb scattering within the bunch [5,6]. In this paper, we further study the beam loss due to multiple scattering with residual gas molecules on a typical normal conducting machine.

Computational Method

Electrons travelling around the machine undergo many small-angle scattering with residual gas molecules. Since the events are completely independent, the resultant scattering distribution is Gaussian, the mean square angle of which is given by [7]

$$\langle\theta^2\rangle \simeq 2\pi N\left(\frac{2Ze^2}{pv}\right)^2 \ln\left(\frac{\theta_{max}}{\theta_{min}}\right) d \qquad \cdots\cdots (1)$$

with

$$\ln\frac{\theta_{max}}{\theta_{min}} \simeq 2\ln(210Z^{-1/3}) , \qquad \cdots\cdots (2)$$

where N is the molecule density, Z is the atomic number of the molecule, p is the electron momentum, v is its velocity, θ_{max} and θ_{min} are the maximum scattering and cutoff angles, respectively, and d is the thickness of gas molecules.

In the actual case, the main components of residual gases are H_2 and CO which are typical in ultra-high vacuum conditions. In view of the dependence of $\langle\theta^2\rangle$ on the atomic number, we assume that the residual gas is all CO. Eq. (1) is then rewritten as

$$\langle\theta^2\rangle \simeq 5 \times 10^5 P_r \delta t/E^2 , \qquad \cdots\cdots (3)$$

where the unit of $\langle\theta^2\rangle$ is rad^2, P_r(Torr) is the residual gas pressure, δt(s) is the travelling time of electrons, E(MeV) is the electron energy, and the value of Z was taken to be 10.

To calculate the beam loss by multiple scattering, the distribution function is described with respect to the beam divergence denoted by x' and y' for the horizontal and vertical directions, respectively. This is the safer side of approximation, since the kick angle of the electron located near the aperture becomes smaller when it is transposed to the x' or y' axis in the phase space. Fig. 1 shows the schematic beam

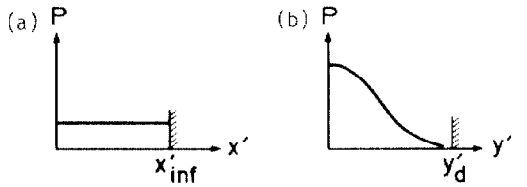

Fig. 1 Schematic beam distributions in the (a) horizontal and (b) vertical directions with respect to the beam divergence right after the multi-turn injection.

distributions with respect to x' and y' right after the multi-turn injection. The beam is almost uniformly distributed in the horizontal direction between the inflector wall and the beam orbit center. The beam divergence at the inflector wall, which corresponds to the physical acceptance, is given by

$$x'_{inf} = x_{inf}/\beta_{x,inf} , \qquad \cdots\cdots (4)$$

where β_x is the horizontal β function and the subscript inf denotes the inflector. As for the vertical direction, the distribution of the injected beam, which is assumed to be Gaussian, is maintained when the physical acceptance given by

$$y'_d = y_d/\beta_{y,max} \qquad \cdots\cdots (5)$$

is sufficiently larger than the dispersion of the injected beam. Here, y_d is the effective value of the duct half height, which is defined as the real size minus COD, and $\beta_{y,max}$ is the maximum vertical β function. When the value of y_d is small, which usually happens in large COD, the injected beam is cut by the duct wall, resulting in a step-like distribution at the wall position.

Starting from these initial conditions, the time dependence of the beam intensity was estimated by taking account of both scattering and damping. The beam intensity in this case is defined by the rate which is left without suffering initial cut in the vertical direction and succeeding scattering beyond the

Present address, ULSI Research Center 1, Komukai-toshiba-cho, Saiwai-ku, Kawasaki

aperture.

The beam distribution function, represented in the x' direction, considering scattering with the residual gas molecules during δt is given by

$$P[x'_1(t+\delta t)] = \int_{-x'_{inf}}^{x'_{inf}} P[x'(t)]\frac{1}{\sqrt{2\pi}\theta} \exp[-\frac{(x'-x'_1)^2}{2\theta^2}]dx' , \quad \ldots\ldots (6)$$

$$\theta^2 = \frac{1}{2}\langle\theta^2\rangle . \quad \ldots\ldots (7)$$

Eq. (7) is used to share the value obtained by eq. (3) between the x' and y' directions. The damping term during δt, again represented in the x' direction, is expressed by the following transformations:

$$x'(t+\delta t) = x'(t)\sqrt{\frac{E(t)}{E(t+\delta t)}}\exp(-\frac{\delta t}{\tau_x}) , \quad \ldots\ldots (8)$$

$$P(t+\delta t) = P(t) / \sqrt{\frac{E(t)}{E(t+\delta t)}}\exp(-\frac{\delta t}{\tau_x}) . \quad \ldots\ldots (9)$$

Here, τ is the radiation damping time which is given in the x and y directions by

$$\tau_x = 1/\frac{U_0}{2ET_0}[1 - \frac{\langle\eta\rangle_b}{\rho}(1-2n)] , \quad \ldots\ldots (10)$$

$$\tau_y = 2ET_0/U_0 , \quad \ldots\ldots (11)$$

respectively, where U_0 is the radiation loss per turn, T_0 is the revolution period, $\langle\eta\rangle_b$ is the mean momentum dispersion in the bending sections, ρ is the bending radius, and n is the magnetic index on the beam orbit. The energy dependence of θ and τ during δt was taken into account in the condition that the beam is linearly accelerated to the final value.

Variable time steps, which are twenty every order, were used in calculating the temporal dependence of the beam intensity. The first step was chosen to be 10^{-4} s after confirming the results obtained with 10^{-4} s and 10^{-5} s to be almost the same. Concerning the mesh numbers in the x' and y' directions, they were both chosen to be 50 after confirming that the results with the meshes of 50 and 200 are almost duplicate.

The residual gas pressure is given by

$$P_r = P_{r0} + \int \zeta_{pd}(E_p)\Phi_p(E_p)dE_p/S , \quad \ldots\ldots (12)$$

where P_{r0} is the static pressure, ζ_{pd} is the photon-impact desorption (photo-desorption) yield with the unit of molecules/photon, Φ_p is the photon flux, E_p is the photon energy, and S is the pumping speed. The mechanism of photo-desorption is that electrons are first emitted from the wall surface under photon irradiation, these electrons hit the wall again, and they desorb the adsorbed gas species on the surface. For the usual wall material (Ex. stainless steel), the lower limit of the photon energy for gas desorption can be taken to be 10 eV (1200 Å). This is because the photons below this energy can hardly emit the secondary electrons of the order of 1 eV which has been considered as the threshold for gas desorption in ultra-high vacuum conditions [8]. Integrating the photon flux above this limit and using the mean desorption yield ζ_d, eq. (12) is expressed as [8]

$$Pr = P_{r0} + \frac{8.08 \times 10^{17} IE[1-(\lambda_c/\lambda_\alpha)^{1/3}]\zeta_d}{3.5 \times 10^{19} s} , \quad \ldots\ldots (13)$$

where λ_c is the characteristic wave length of synchrotron radiation, λ_α is the above-mentioned threshold photon energy denoted by the wave length, and the units of P_r, I, E and S are Torr, A, MeV and ℓ/s, respectively. Although eq. (13), strictly speaking, is applicable in $\lambda_c/\lambda_\alpha \lesssim 1/3$, it is useful to show the general trend that photo-desorption arises in the energy corresponding to $\lambda_c \sim \lambda_\alpha$ in the process of acceleration and increases with beam energy.

Results and Discussion

Table 1 shows the parameters of the machine studied in this paper. Electrons are injected in 15 MeV and accelerated to the final energy, 800 MeV, in 100 s. The bending magnetic field is 1.5 T in 800 MeV, the bending angle per one sector-type magnet is 90°, and the magnetic index is 0.4 on the electron orbit. The circumference of the orbit is 21 m which is rather small for 800 MeV machines. Table 2 shows the detailed

Table 1 Ring parameters

Injection energy	15 MeV
Stored energy	800 MeV
Acceleration time	100 s
Stored current	500 mA
Bending field	1.5 T
Magnetic index	0.4
Circumference	21 m
Horizontal tune	1.28
Vertical tune	0.617
Rf frequency	114 MHz
Rf voltage	3 kV at 15 MeV 100 kV at 800 MeV
Pressure	1×10^{-9} Torr at 15 MeV 4×10^{-9} Torr at 800 MeV

ring parameters concerning beam loss calculation. The inflector wall is located at x = 35 mm, and β_x and the momentum dispersion, η, at the inflector are both 2.2 m. As for the vertical direction, the maximum β is 6.6 m, and the duct size is 30 mm. Table 3 shows

Table 2 Detailed parameters for beam loss calculation

Inflector location	x = 35 mm
β_x at the inflector	2.2 m
η at the inflector	2.2 m
Maximum β_y	6.6 m
Vertical duct size	30 mm

the beam parameters of an injector linac with a suitable energy compression system. The beam divergence, which is the most critical parameter in this estimation, is 1 mrad. Analysis on multi-turn injection has shown that about 10 turns of the beam can be effectively injected in the conditions shown in tables 1 to 3 [3]. Assuming the capture efficiency in the bunching process to be 50%, the designed maximum stored current of this machine is 500 mA.

Table 3 Injected beam parameters

Beam current	100 mA
Beam diameter	4 mm
Beam divergence	1 mrad
Energy spread	±0.5%

Fig. 2 shows the temporal change of the horizontal beam profile during 8.9 s after the injection. It is indicated that the ribbon-like beam shrinks without suffering any kick-off beyond the inflector wall after the injection. This is because the adiabatic damping term of off-axis beam is comparatively large, since the damping term is proportional to x' as was shown in eq. (8). It was confirmed that the behavior of beam shrinkage does not change for a possible COD (∿5 mm)

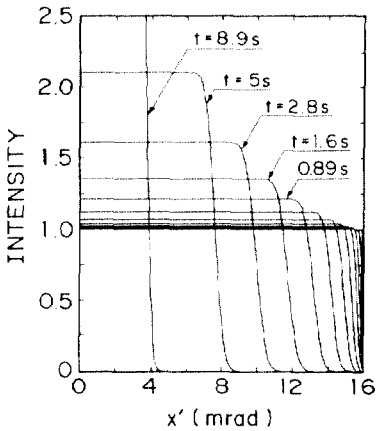

Fig. 2 Temporal change of the horizontal beam profile during 8.9 s after the injection

in the x direction. The CO pressure used in this estimation is 10^{-9} Torr, since photo-desorption is negligible during this period (the beam energy is still below 95 MeV corresponding to $\lambda_c = 1.16 \times 10^4$ Å).

Fig. 3 shows the temporal change of the vertical beam profile during the first 8.9 s for y_d = 15 mm and 5 mm. When the COD is zero, namely y_d = 15 mm, the injected beam is completely included in the duct and starts shrinking right after the injection. This is again because the adiabatic damping exceeds the scattering due to residual gases in large y'. When the COD is 10 mm (corresponding to y_d = 5 mm), which was assumed to be larger than the horizontal one because of $\beta_{y,max} = 3\beta_{x,inf}$, the acceptance in the y' direction is only 0.76 mrad. In this case, the beam is cut by the duct wall in the first turn after the injection, and the scattering term exceeds the adiabatic damping term till t = 5 s. The radiation damping then becomes comparable to the scattering, and the beam starts shrinking.

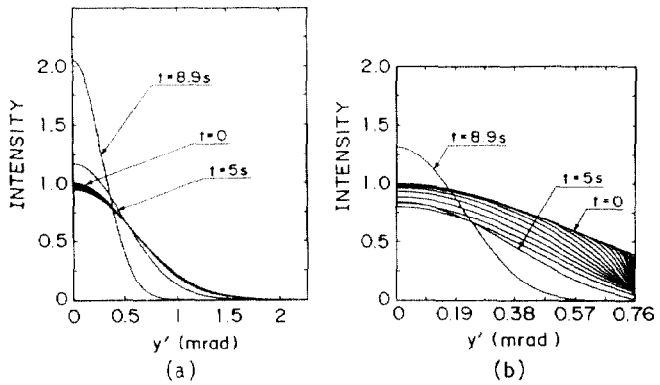

Fig. 3 Temporal change of the vertical beam profile during 8.9 s after the injection for (a) y_d = 15 mm and (b) y_d = 5 mm.

Fig. 4 shows the temporal dependence of the beam intensity during the first 8.9 s for various y_d values. The beam cut in the first turn explained in Fig. 3b happens in $y_d \lesssim 10$ mm. The beam intensity at t = 0 s including this effect is 99, 92, 69 and 25% for y_d = 10, 7.5, 5 and 2.5 mm, respectively. Although almost no beam is lost in $y_d \gtrsim 12.5$ mm, general trend is that the beam intensity decays for about 5 s till the radiation damping becomes to exceed the scattering with residual gases. Since the COD is expected to become less than 2 mm by operating correction magnets, almost all the beam appears to survive after the COD correction.

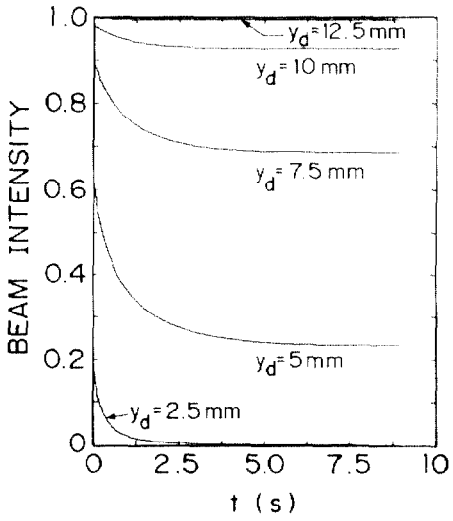

Fig. 4 Temporal dependence of the beam intensity during 8.9 s after the injection.

When the beam energy passes through 200 MeV in the acceleration process, the residual gas pressure starts to increase because of photo-desorption, as was shown in eq. (13). The vacuum system to be installed in the machine has a capability to achieve 4×10^{-9} Torr in E = 800 MeV and I = 500 mA when the duct wall is throughly cleaned by photon irradiation. The value of ζ_d assumed for this design condition is 5×10^{-6} molecules/photon. The ζ_d, however, can be as high as 10^{-3} when the duct wall is dirty, namely in initial operation of the machine. Eq. (13) shows that the upper limit of the pressure in 200 MeV for this dirty condition is 6×10^{-8} Torr for I = 500 mA. Beam scattering behavior for these conditions was estimated and showed that no beam loss is expected due to multiple scattering with residual gases, since the scattering angle during the term of τ_y in 200 MeV (0.4 s) is much less than the physical acceptance denoted by the divergence. We have also estimated the effect of large angle single scattering with residual gases. It was confirmed that the beam loss during acceleration with this effect is less than 1% in $\zeta_d = 5 \times 10^{-6}$ and about 20% in $\zeta_d = 10^{-3}$.

In conclusion, the beam loss due to multiple scattering with residual gases was studied in the storage-type electron synchrotron, the injection energy of which is 15 MeV and the acceleration time to 800 MeV is 100 s. It was found that the beam loss due to the multiple scattering depends on the value of vertical COD and can be reduced to the negligible level when the COD is corrected.

References

[1] G. Rakowsky, IEEE Trans. NS-32 (1985) 2377.
[2] U. Trinks, F. Nolder and A. Jahnke, Nucl. Instr. and Meth. 200 (1982) 475.
[3] K. Nakayama and Y. Gomei, European Particle Accelerator Conf. (World Scientific, Singapore) 573.
[4] K. Nakayama and Y. Gomei, Rev. Sci. Instr. 60 (7), (1989) 1756.
[5] Y. Gomei and K. Fukushima, Nucl. Instr. and Meth. A262 (1987) 534.
[6] Y. Gomei, K. Nakayama, K. Fukushima and S. Sukenobu, ibid A 278 (1989) 389.
[7] J. D. Jackson, Classical Electrodynamics (John Wiley & Sons, Inc., 1962) P. 456.
[8] M. Bernardini and L. Malter, J. Vac. Sci. Technol. 2 (1965) 130.